

UNCLASSIFIED

Defense Technical Information Center
Compilation Part Notice

ADP014243

TITLE: Microstructures and Mechanical Properties of Nanostructured Copper-304 Stainless Steel Multilayers Synthesized by Magnetron Sputtering

DISTRIBUTION: Approved for public release, distribution unlimited

This paper is part of the following report:

TITLE: Materials Research Society Symposium Proceedings Volume 740
Held in Boston, Massachusetts on December 2-6, 2002. Nanomaterials for Structural Applications

To order the complete compilation report, use: ADA417952

The component part is provided here to allow users access to individually authored sections of proceedings, annals, symposia, etc. However, the component should be considered within the context of the overall compilation report and not as a stand-alone technical report.

The following component part numbers comprise the compilation report:
ADP014237 thru ADP014305

UNCLASSIFIED

Microstructures and Mechanical Properties of Nanostructured Copper-304 Stainless Steel Multilayers Synthesized by Magnetron Sputtering

X. Zhang, A. Misra, H. Wang, H. Kung, J. D. Embury, R. G. Hoagland and M. Nastasi
Materials Science and Technology Division, Mail Stop G755, Los Alamos National Laboratory,
Los Alamos, NM 87545

Abstract

Nanostructured Cu/304 stainless steel (SS) multilayers were prepared by magnetron sputtering at room temperature. 304SS has a face-centered cubic (fcc) structure in bulk. However, in the Cu/304SS multilayers, the SS layers exhibited fcc structure for layer thickness of less than or equal to 5 nm. For 304SS layer thickness larger than 5nm, bcc 304SS grains were observed to grow on top of the initial ≈ 5 nm of fcc SS. The maximum hardness of Cu/304SS multilayers was ≈ 5.5 GPa (factor of two enhancement compared to rule of mixtures hardness) achieved at a layer thickness of 5nm, with a decrease in hardness with decreasing layer thickness below 5 nm. The hardness of fcc/fcc Cu/304SS multilayers (layer thickness ≤ 5 nm) is compared with Cu/Ni, another fcc/fcc system, to gain insight on how the mismatch in physical properties such as lattice parameters and shear moduli of the constituent layers affect the peak hardness achieved in these nanoscale systems.

Introduction

Nanostructured multilayers are made up of alternating nanometer scale layers of two different materials. The layer thickness can be well controlled in the scale of 1nm or less by physical vapor deposition (PVD). These nanostructured multilayers have novel mechanical, electrical, magnetic, and optical properties [1-3]. The mechanical properties of these multilayered composites are of particular interest since the strength of these multilayer composites can be significantly increased to about 1/3 of the theoretical strength limit [4]. In the μm to the sub- μm length scale regime, the strengthening in these multilayers can be explained by the Hall-Petch model of dislocation pile-ups at interfaces or grain boundaries. The yield strength, σ_y , is proportional to $h^{-1/2}$, where h is the layer thickness [5,6]. Hall-Petch slope is a measure of the strength of interface barrier for dislocation pile-ups and determines the rate of strength increase with decreasing h . However, in the tens of nanometers regime the Hall-Petch model breaks down [1]. The deformation mechanism may involve glide of single dislocations, in the form of Orowan loops, leading to $\sigma_y \propto \ln(h)/h$ relation [4,7]. In the limit of a few nanometers, the strength of the multilayer may be determined by the stress to transmit a single dislocation across the interfaces. Factors such as shear modulus mismatch and lattice parameter mismatch may determine the transmission stress for single dislocations. For multilayers with a large difference between shear modulus, dislocations in the low shear modulus phase need to overcome a high repulsive stress (Koehler stress) to enter the high modulus phase [8]. Furthermore, coherency stresses within the thin lattice matched multilayers may alternate from tensile to compressive in adjacent layers, and results in an additional barrier for single dislocation transmission across interfaces [9, 10]. The magnitude of coherency stress increases with increasing lattice parameter mismatch. When the interfaces are semi-coherent, the spacing of the misfit dislocations at the interface reduces with increasing lattice parameter mismatch. In some systems, a drop in strength, or softening, is observed [1, 11-13] when the layer thickness is below a few nanometers. The mechanisms for this softening, however, are not well understood.

In this paper, we report the studies on microstructures and mechanical properties of Cu/304SS multilayers. It is previously known that the Cu/304SS multilayers have fcc/bcc structure for a layer thickness larger than 5 nm, while they have fcc/fcc structure for a layer thickness less than 5 nm [14]. At layer thickness of less than 5nm, a reasonable comparison can be made between Cu/304SS and Cu/Ni multilayers to understand the effects of lattice parameter mismatch on the peak hardness. A comparison of mutual solubility, interface misfit and Young's modulus mismatch between Cu/304SS and Cu/Ni (single crystal with cube on cube orientation) is listed in Table 1.

Table 1. A comparison of Cu/304SS ($h \leq 5$ nm) with Cu/Ni multilayer system.

Materials	Mutual solubility	Crystal structure	Lattice parameter mismatch*	E_X/E_{Cu} **
Cu/Ni [11]	completely miscible	fcc/fcc	2.63%	1.99
Cu/304SS	major elements immiscible with Cu [^]	fcc/fcc	0.48% (fcc SS)	1.82

[^] Cu may have limited solubility in fcc SS [15]

* For fcc/fcc systems, % misfit between interplanar spacing of {100}.

** E_{Cu} is the average Young's modulus of polycrystalline Cu and E_X is the average Young's modulus of the other phases. For Cu, Ni, the ratio of the Young's modulus in (100) orientation is calculated.

Experimental

Cu/304SS multilayers were DC sputter deposited at room temperature on Si (100) substrates that have a native SiO₂ layer. The chamber was evacuated to a base pressure of $\leq 5 \times 10^{-8}$ torr prior to deposition. Ar pressures of 5 mtorr and 4mtorr were used for the deposition of 304SS and Cu respectively. Sputtering power of 200W and 100W for 3.95 inch diameter targets were used for the deposition of 304SS and Cu respectively. In all multilayered composites, 304SS was always deposited as the first layer on Si substrate. The thickness of the constituent layers within the multilayers was varied from 1 to 500 nm, and the total number of bilayers deposited was such that the total multilayer film thickness was ≈ 2 μ m. Transmission electron microscopy (TEM) was performed on a Philips CM30 microscope at 300kV. The hardness and indentation modulus of the multilayers and 2 μ m single layered Cu and 304SS films were measured using an indentation load-depth sensing apparatus, commercially available as Nano Indentor II. Continuous stiffness technique was used for nano-indentation with a displacement rate of 2 nm/s. The nominal indentation depth was 250 nm.

Results and Discussions

Microstructures of Cu/304SS multilayers are studied systematically for all layer thickness with TEM. Selected examples are given in the sequence of increasing layer thickness beginning with the smallest layer thickness of 1nm. Fig. 1 shows that Cu/304SS multilayers with 1 nm layer thickness exhibits a sharp interface between each layer. Columnar grain size, on the average of 33 nm, within each layer is much greater than the layer thickness. The corresponding selected area diffraction pattern (inset in Fig. 1) shows a weak {111} fiber texture for the 304SS



Cu/304SS multilayers with layer thickness ≤ 5 nm also exhibited fcc structures in both layers. At layer thickness ≥ 10 nm (Fig. 2), additional diffraction rings corresponding to bcc 304SS (lattice parameter = 0.2866 nm) were also observed. Dark field TEM, not shown here, revealed that the initial ≈ 5 nm thick 304SS from the Cu/304SS interface was fcc and then bcc 304SS grains grew on top of the fcc grains. Thus, higher layer thickness multilayers exhibited predominantly bcc grains (as shown in Fig. 3 for Cu/304SS 100 nm sample) with the much smaller fcc grains confined to the interfacial region. The formation of bcc 304SS is nevertheless a surprising result since 304 austenitic SS has 8-10 % Ni to stabilize the fcc austenite phase.

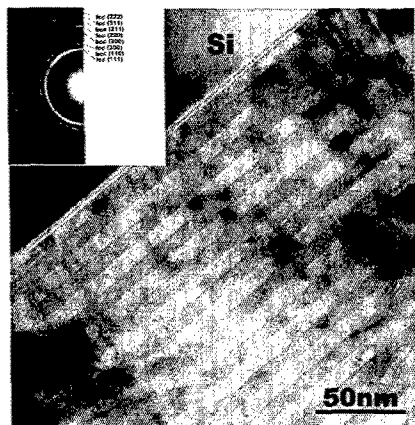


Fig. 2. Bright field TEM micrograph of Cu/304SS multilayers with a layer thickness of 10nm. Compared to Fig. 1, the diffraction pattern shows additional rings from the bcc structure of 304SS.

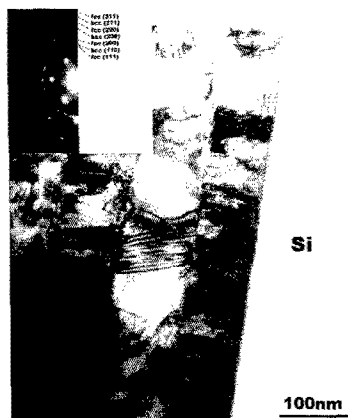


Fig. 3 Bright field TEM micrograph showing the cross section of Cu/304SS multilayers with 100 nm layer thickness. Diffraction pattern (similar to Fig. 2) shows a mixture of bcc and fcc 304SS phases, along with fcc Cu.

The formation of metastable bcc 304SS thin film is proposed to be due to the rapid vapor quenching achieved in the sputtering process [16]. It is speculated that the fcc structure in sputtered 304SS thin films can only be stabilized by epitaxial growth on fcc Cu underlayer [14]. However, we have observed fcc structure in the first few nanometers of the 304SS thin film sputter deposited on other non-fcc substrates as well, e.g., Si with native oxide. It is possible that dc magnetron sputtering of an alloy target that contains primarily Fe, Ni and Cr may not result in a film with identical composition to the target. For 304SS, even a small drop in the Ni to Fe ratio with increasing thickness may lead to the stabilization of the bcc structure. We are investigating this in more detail using Auger depth profiling of the film composition as well as sputtering other austenitic stainless steels that have higher Ni concentration to see what structures are obtained in the thin films, and will report the findings in a separate article later.

The hardness of Cu/304SS and Cu/Ni multilayers are plotted as a function of $h^{-1/2}$ (Hall-Petch plot) in Fig. 4, where h is the layer thickness. Hardness of Cu/304SS multilayers increased almost linearly with $h^{-1/2}$ for $h \geq 100\text{nm}$, consistent with the Hall-Petch model. This linear relationship is deviated at smaller layer thickness. A maximum hardness of around 5.5 GPa is reached at $h = 5\text{nm}$. For lower h , hardness drops with decreasing layer thickness, reducing to around 4.7 GPa at $h = 1\text{nm}$. The dashed line corresponding to a hardness value of 2.95 GPa represents the rule of mixtures (ROM) values, i.e., average of the hardness of single layered Cu and 304SS films. Therefore, the maximum hardness of multilayers is around a factor of 2 higher than the ROM hardness. Since 304SS has a mixture of bcc and fcc phases at layer thickness larger than 5nm, a demarcation line is drawn in Fig. 4 to separate the plot into two regimes. The first regime, $h > 5\text{nm}$, consists of a mixture of fcc and bcc 304SS phases, while in the second regime, $h \leq 5\text{nm}$, 304SS has fcc phase.

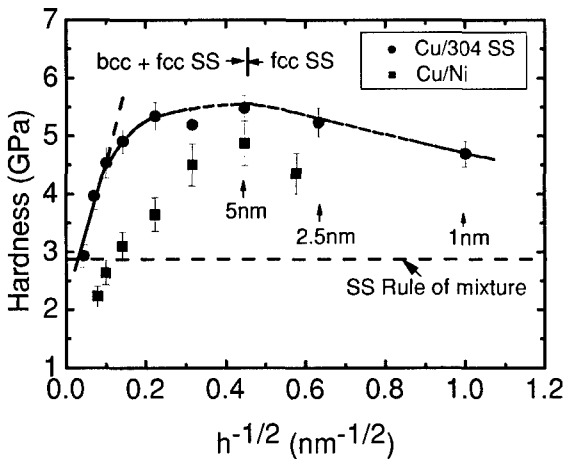


Fig. 4. Hardness of Cu/304SS and Cu/Ni multilayers as a function of $h^{-1/2}$ (h stands for layer thickness). The horizontal dashed line indicates the hardness of Cu/304SS according to the rule of mixtures.

A comparison of mechanical properties of Cu/304SS with previously studied Cu/Ni is listed in table 2, for $h \leq 5$ nm. The ratio of the maximum yield strength, σ_{\max} (estimated as 1/3 of the maximum hardness), to the rule of mixture strength, σ_{rom} , is higher for Cu/304SS as compared to Cu/Ni. Cu/Ni multilayer is expected to be stronger than Cu/304 SS primarily due to a factor of about 5 times larger lattice parameter mismatch. One difference between the two systems that may affect the stress state at the interface is the mutual solubility. Cu and Ni are completely miscible, while Cu and major elements (Fe, Cr) in 304SS are almost immiscible. Therefore the interface between Cu and 304SS could be chemically sharper compared with Cu/Ni. It has been shown that intermixing at the interface over a few monolayers may reduce the interface barrier stress for slip transmission [17]. Another factor that should be taken into account is the crystallinity of the multilayers. Cu/Ni data in Table 2 is for single crystal multilayers with cube-on-cube orientation, while Cu/304SS multilayers were polycrystalline with $\langle 111 \rangle$ texture. For coherent Cu-Ni multilayers, MD simulations have shown that the interface barrier stress is higher for $\{111\}$ twin interfaces than $\{001\}$ interfaces [10]. A comparison between epitaxial single crystalline Cu/SS304 with Cu/Ni, both with (100) orientation, shall be very valuable for further studies of strengthening mechanism at small layer thickness.

Table 2. A comparison of mechanical properties between Cu/304SS ($h \leq 5$ nm) and Cu/Ni multilayers.

Materials	Crystal structure	$\sigma_{\max}/\sigma_{\text{rom}}$	h at σ_{\max} (nm)	Softening
Cu/Ni [11]	fcc/ fcc single crystal (100)	1.61	5	Yes, for $h < 5$ nm
Cu/304SS	fcc/fcc polycrystalline $\langle 111 \rangle$ texture	1.88	5	Yes, for $h < 5$ nm

The similarity between the two systems is that softening occurred at layer thickness of less than 5 nm. It is suspected that softening observed in Cu/Ni could be related to intermixing at the interface between [16]. As mentioned above, graded interface may have lower barrier strength to dislocation transmission than chemically sharp interface. As the layer thickness decreases to a couple nanometers, the ratio of the intermixed layer at the interface (presumably a few monolayers) to the layer thickness increases and this may account for the drop in the strength with decreasing layer thickness below ~ 5 nm. In the case of Cu/304SS, the major elements (Fe, Cr) in fcc 304SS are immiscible with Cu. However, Cu is reported to have $\sim 4\%$ solubility in fcc 304 SS [15] and this may lead to limited intermixing, although much less than the case of completely miscible Cu-Ni system. Furthermore, softening has been observed in immiscible systems as well, although at layer thickness below $\sim 1-2$ nm. Therefore, other factors should be considered in explaining the softening in Cu/304SS multilayers. The absence of misfit dislocations at smaller layer thickness may lower the interface barrier to dislocations [10]. Recent molecular dynamics simulations [18] have shown that softening is to be expected when dislocation core width is some fraction of the layer thickness. Our future work will examine the softening at the smallest layer thicknesses in more detail.

Summary

Sputter-deposited Cu/304SS multilayers have fcc Cu/fcc 304SS structure for a layer thickness less than 5 nm, while a mixture of bcc and fcc 304SS with fcc Cu is observed at larger layer thickness. The maximum hardness of Cu/304 SS is 5.5 GPa, approximately a factor of two higher than the rule of mixtures hardness. The peak hardness of Cu/304SS is higher than that of Cu/Ni multilayer even though the latter has a much larger lattice parameter mismatch, and slightly higher shear modulus mismatch. This may be attributed to lowering of interface barrier stress to single dislocation transmission due to intermixing at the miscible Cu-Ni interface, and to the differences in the texture in these systems. The decrease in hardness when the layer thickness is reduced from 5 to 1 nm needs to be investigated in more detail.

Acknowledgement

This research is funded by DOE-OBES. XZ acknowledges support from LANL director's funded post-doctoral fellowship. Technical assistance from Caleb Evans and Mark Hollander on sputter deposition is acknowledged.

References

1. B. M. Clemens, H. Kung, S. A. Barnett, *MRS Bulletin*, **24**, 20 (1999).
2. P. M. Anderson, T. Foecke, P. M. Hazzledine, *MRS Bulletin*, **24** (1999) 27.
3. G. S. Was, T. Foecke, *Thin Solid Films*, **286**, 1 (1996).
4. J. D. Embury and J. P. Hirth, *Acta Metall. Mater.*, **42**, 2051 (1994).
5. E. O. Hall, *Proc. Roy. Soc. (London)*, **B64**, 474 (1951).
6. N. J. Petch, *J. Iron Steel Inst.*, **174**, 25 (1953).
7. W. D. Nix, *Mater. Sci. Engg.*, **A234-236**, 37 (1997).
8. J. S. Koehler, *Phys. Rev. B.*, **2**, 547 (1970).
9. M. Shinn, L. Hultman, S. A. Barnett, *J. Mater. Res.*, **7**, 901 (1992).
10. S. I. Rao, P. M. Hazzledine, *Phil. Mag. A*, **80**, 2011 (2000).
11. A. Misra and H. Kung, *Adv. Eng. Mater.*, **3**, 217 (2001).
12. P. M. Hazzledine and S. I. Rao, *MRS Symp. Proc.* **434**, 135 (1996).
13. D. M. Tench, J. T. White, *J. Electrochem. Soc.*, **138**, 3757 (1991).
14. K. Parvin and S. P. Weathersby, T. W. Barbee, Jr., T. P. Weihs and M. A. Wall, *Mater. Res. Soc. Symp. Proc.*, **382**, 191 (1995).
15. Jacek Banas, Andrzej Mazurkiewicz, *Mater. Sci. Engg.*, **A**, **277**, 183 (2000).
16. T. W. Barbee, B. E. Jacobson, and D. L. Keith, *Thin Solid Films*, **63**, 143 (1979).
17. X. Chu and S. A. Barnett, *J. Appl. Phys.*, **77**, 4403 (1995).
18. R. G. Hoagland, T. E. Mitchell, J. P. Hirth and H. Kung, *Phil. Mag. A*, **82**, 643 (2002).

Poster Session